

Simulation of Diffusion Mechanism and Dynamics in Alumina Liquid under Pressure

Nguyen Thi Thanh Ha*, Pham Khac Hung

*Department of Computational Physics, Hanoi University of Science and Technology
1 Dai Co Viet, Hanoi, Vietnam*

Received 05 January 2013

Revised 25 February 2013; accepted 18 March 2013

Abstract: Diffusion mechanism and dynamics in Al_2O_3 liquid have been studied via molecular dynamics simulation. Six models with different density and at temperature of 3000 K have been used to study the atomistic mechanism governing the process of the bond-breaking and bond-reformation (the transition $\text{AlO}_x \rightarrow \text{AlO}_{x+1}$ and $\text{AlO}_x \rightarrow \text{AlO}_{x-1}$). Calculation shows that the diffusion of particle Al is realized via the transition $\text{AlO}_x \rightarrow \text{AlO}_{x\pm 1}$ and the rate of transition $\text{AlO}_x \rightarrow \text{AlO}_{x\pm 1}$ monotonously increases with pressure. When applying pressure to liquid the diffusion mechanism changes from strong localization of transitions $\text{SiO}_x \rightarrow \text{SiO}_{x\pm 1}$ in the sample at ambient pressure to uniform distribution transitions $\text{SiO}_x \rightarrow \text{SiO}_{x\pm 1}$ in high-pressure sample. Furthermore, we find two distinguish regions with quite different coordination environment where the rate of transitions $\text{SiO}_x \rightarrow \text{SiO}_{x\pm 1}$ strongly differs from each other. The result obtained clearly evidences the spatially heterogeneous dynamics in the liquid.

1. Introduction

Recently, the dynamics in network-forming liquid continues to attract a great interest among the researchers in the field of material science. The problem debated for long time is the dynamics heterogeneity (DH) [1-3]. In the system displaying DH there are distinguish regions where the mobility of particles is fast or slow. The fast and slow regions migrate over time in the space. DH has been detected by two- and four-point dynamical correlation function [4] and is visualized through simulation for the soft-sphere systems [5], hard-sphere systems [6] and Lennard-Jones (LJ) systems [7]. Experimentally, DH is detected for fragile liquids [8] and for colloidal dispersions using particle-tracking technique [9].

Several theories have been proposed to interpret the phenomena mentioned above. The Adam-Gibbs approach [10] sees the glass transition phenomenon as resulting from an increase of

* Corresponding author. Tel.: 84-983012387
E-mail: thanhha12386@yahoo.com

cooperatives of molecular dynamics upon cooling. Very recently, Garrahan and Chandler (GC) [11] introduced a microscopic model of super-cooled liquids, which is based on two important points: (i) Particle mobility is sparse and dynamics are spatially heterogeneous at times intermediate between ballistic and diffusive motion. (ii) Particle mobility is the result of dynamic facilitation, i.e., mobile particles assist their neighbors to become mobile [12]. Furthermore, it was shown that a group of particles follows one another along string-like paths [13]. However, the physical mechanism behind this phenomenon has not been successfully identified in these studies.

Alumina is an important ceramic material and has many technological applications, from electronics, optics, biomedical and mechanical engineering [14]. So, the knowledge of the structure and dynamics at atomic level would be an important step towards understanding this material. As shown from previous studies the spatial distribution of transitions $MO_x \rightarrow MO_{x\pm 1}$ (SDT) strongly affects the diffusivity in the disordered systems [15]; here M is cation. Hence, the specific behavior of dynamics in alumina liquid may be originated from SDT, but this problem is not studied yet. This motivated us to perform a systematic study on the microstructure and dynamics of alumina liquid on base of transition $AlO_x \rightarrow AlO_{x\pm 1}$.

2. Calculation method

The Al_2O_3 liquid has been studied via molecular dynamics method, which applied here can be found elsewhere [16,17]. The model MD of liquid Al_2O_3 is carried out containing 2000 atoms with periodic boundary conditions. The Born-Mayer type pair potential used here is given as [17]

$$u_{ij}(r) = z_i z_j \frac{e^2}{r} + B_{ij} \exp\left(-\frac{r}{R_{ij}}\right) \quad (1)$$

The long-range Coulomb interactions are calculated with the standard Ewald summation technique. The Verlet algorithm with a time step (MD step - t_{MD}) of 0.47 fs was adopted. Initial configuration was generated by random placing all atoms in a simulation box with sizes of 29.03 Å under the constraint that the distance between every two pairs is higher than a specified value. This configuration is heated to 5000 K. A well-equilibrated liquid model (M1) has been constructed at temperature of 3000 K and at ambient pressure. We prepare four other models (M2-M6) by compressing model M1 to desired density and consequent long relaxing in N-P-T ensemble (constant temperature and pressure) until reach equilibrium. We also perform a long relaxation in N-E-V ensemble (constant volume and energy) to obtain well-equilibrated sample and collect the dynamical quantities.

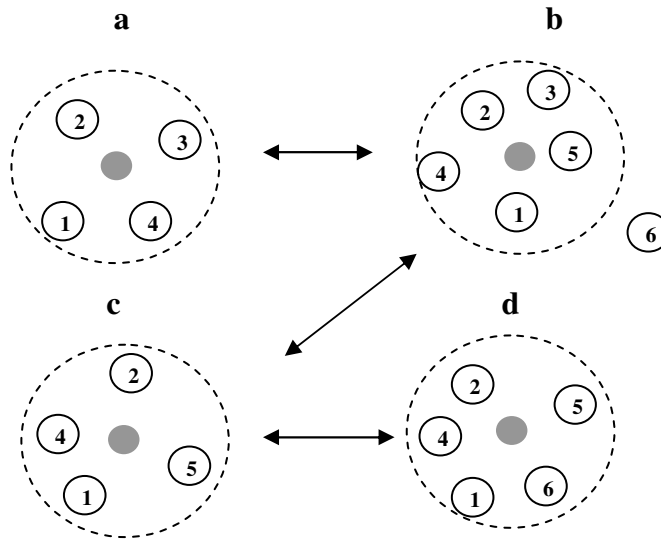


Fig. 1. Schematic illustration of diffusion mechanism in Al_2O_3 liquid; (a, c) structural units AlO_4 and (b, d) structural units AlO_5 .

The diffusion of the Al atoms was performed via the breaking and reforming of structural units AlO_x ($x=4, 5, 6$). The number of transitions $\text{AlO}_4 \rightarrow \text{AlO}_6$ and $\text{AlO}_6 \rightarrow \text{AlO}_4$ are very small so that these can be ignored. Hence, we consider only the transitions $\text{AlO}_4 \rightarrow \text{AlO}_5$ and $\text{AlO}_5 \rightarrow \text{AlO}_4$ ($\text{AlO}_x \rightarrow \text{AlO}_{x+1}$) as shown in Fig. 1. These transitions can be viewed such as two types: The first one creates a new stage of AlO_x (see in Fig. 1: $a \rightarrow b \rightarrow c$), and the second one is a back-forth transition which restores the previous state (see in Fig. 1: $a \rightarrow b \rightarrow a$ or $c \rightarrow b \rightarrow c$ or $c \rightarrow d \rightarrow c$). m_{trans} is a number of transitions $\text{AlO}_x \rightarrow \text{AlO}_{x \pm 1}$ occurred within the time.

The diffusion coefficient of particles in MD model is usually determined

$$D = Av_{trans}d_{trans} \tag{2}$$

$$\text{Where } A = \frac{1}{6t_{MD}}; \quad d_{trans} = \lim_{m_{trans} \rightarrow \infty} \frac{\langle r(t)^2 \rangle}{m_{trans}}; \quad v_{trans} = \frac{m_{trans}}{n} \tag{3}$$

Where n is number of MD steps; t_{MD} is MD step, $t=nt_{MD}$; v_{trans} is a rate of transition $\text{AlO}_x \rightarrow \text{AlO}_{x \pm 1}$; The cutoff distance used to calculate the coordination number is 2.54 \AA .

3. Result and discussion

3.1. The mechanism of diffusion

The firstly, modeling results are compared to experimental data, and therefore allow us to test the reliability of models. The total radial distribution function (RDF) $g(r)$ of model M1 and experiment [18] is shown in Fig. 2. It can be seen that the curves fit well the positions of two peaks and our

calculated $g(r)$ is in good agreement with the experimental one. The distribution of coordination number calculated here shows that the liquid transforms from tetrahedral to octahedral network structure as the pressure varies from zero to 20 GPa. This result is also in good agreement with previous study.

Table 1. C_4 , C_5 are the fraction of four- and five-fold coordination, respectively. $C_{6+other}$ is total fraction of six coordination and another type coordination (3 or 7)

Model	M1	M2	M3	M4	M5	M6
Pressure., K	-0.15	2.96	6.37	11.22	15.89	20.47
C_4	0.67	0.54	0.41	0.29	0.20	0.14
C_5	0.27	0.40	0.47	0.52	0.52	0.50
$C_{6+other}$	0.06	0.07	0.11	0.19	0.28	0.37

Fig.1 shows for instance the coordination evolution. We can see that the particle Al undergoes three stages AlO_4 , AlO_5 and AlO_6 with two transitions $AlO_4 \rightarrow AlO_5$ and $AlO_5 \rightarrow AlO_6$. The time separation between transitions shown in Fig.1 is the lifetime of the stage AlO_5 . Important quantity characterized the dynamics is the mean lifetime AlO_x . We denote τ_4 , τ_5 , τ_6 and τ_{other} to the mean lifetime of stages AlO_4 , AlO_5 , $AlO_{6+other}$ of all stages AlO_x . Obviously, $v_{trans}^{**} = \tau_x^{-1}$.

In Fig.3 we show the lifetime of stage AlO_x as a function of pressure. For low-pressure sample we see a significant large value of τ_4 compared to other types of lifetime AlO_x that indicates most stable unit AlO_4 in the low-pressure liquid. Meanwhile, for high-pressure sample the unit AlO_6 is most stable, and therefore we observe the monotonous increase in τ_6 (see Fig.3). The average lifetime τ_x in contrast, decreases with increasing the pressure.

Table 2 show the value of v_{trans}^* and d_{trans} of alumina liquid under pressure. v_{trans} (rate of transition $AlO_x \rightarrow AlO_{x\pm 1}$) is determined by means of slope of dependence m_{trans} on step n ; d_{trans} is determined by means of slope of dependence $\langle r(t)^2 \rangle$ on m_{trans}

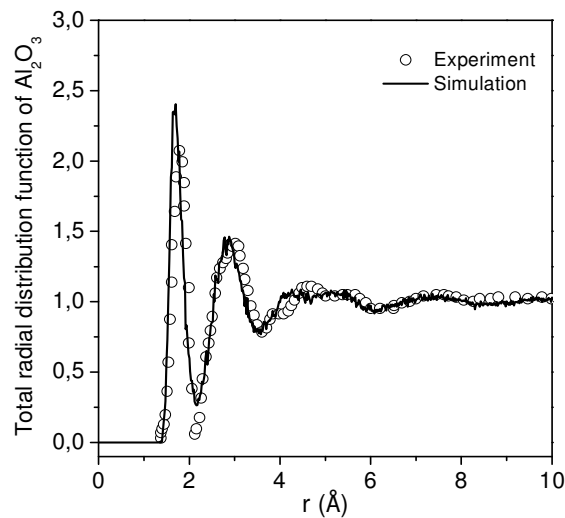


Fig. 2. Total RDF of liquid Al_2O_3 model M1 ($T = 3000$ K and $P = 0$ GPa) and experimental [18] data in Ref.

Model	M1	M2	M3	M4	M5	M6
Pressure. GPa	-0.15	2.96	6.37	11.22	15.89	20.47
$v_{trans}^* \cdot 10^{-3}$	4.87	6.27	7.44	8.72	9.82	10.52
$v_{trans}^{**} \cdot 10^{-3}$	4.89	6.28	7.47	8.74	9.83	10.55
$d_{trans}, \text{\AA}^2$	0.06	0.04	0.03	0.02	0.02	0.01

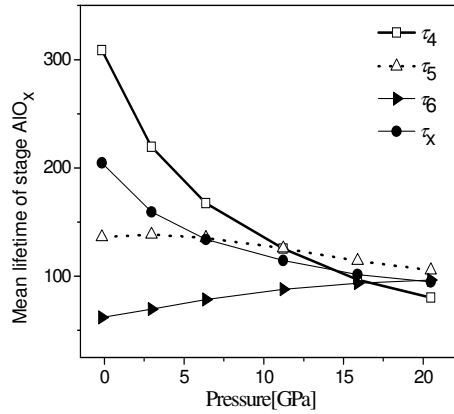


Fig.3. The pressure dependence of averaged lifetime of stage AlO_x .

The monotonous increase of v_{trans} with increasing pressure again indicates most stable units AlO_4 at ambient pressure. This implies that the Al-O bond is weaker under pressure. The pressure dependence of d_{trans} is more complicated due to that it strongly depends on the spatial distribution of $AlO_x \rightarrow AlO_{x\pm 1}$.

The diffusion constant plotted in Fig.4 for different pressure shows a good agreement between data calculated by Einstein equation $D = \lim_{t \rightarrow \infty} \frac{\langle r(t)^2 \rangle}{6t}$ (4) and via parameters v_{trans} and d_{trans} in accordance to Eq.(2). From above results, one time again it demonstrates that the diffusion mechanism in liquid alumina is realized by the change of nearest-neighbor atoms amongst coordination units. In other word, the diffusion mechanism in liquid Al_2O_3 is based on the transition $AlO_x \rightarrow AlO_{x\pm 1}$. The diffusivity of alumina occurs when there is a change in the coordinated oxygen of AlO_x .

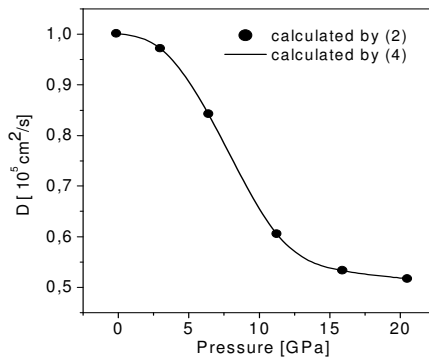


Fig.4. The pressure dependence of coefficient diffusion for Al_2O_3 .

The change in diffusion coefficient under pressure can be expressed as

$$\eta_D = \frac{D(P)}{D(0)} = \frac{v_{trans}(P)}{v_{trans}(0)} \frac{d_{trans}(P)}{d_{trans}(0)} = \eta_{trans} \eta_{dtrans} \quad (5)$$

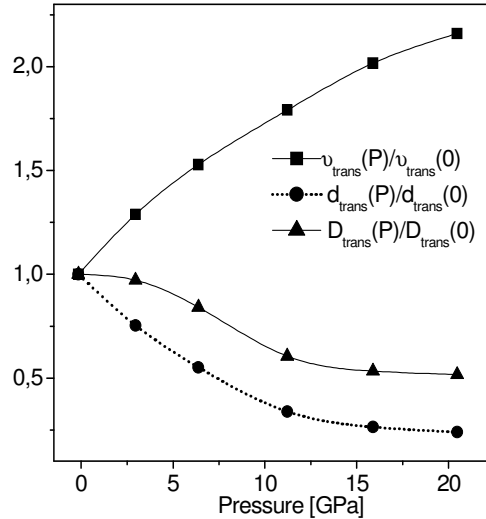


Fig.5. The dynamical quantities for Al_2O_3 liquid.

Thus η_D can be expressed by two terms. The first one relates to the transition frequency of $\text{AlO}_x \rightarrow \text{AlO}_{x\pm 1}$ which is strongly correlated with the change in statistic properties of liquid. The second term depends on the spatial distribution of $\text{AlO}_x \rightarrow \text{AlO}_{x\pm 1}$. In Fig.5 we show the η_{trans} and η_{dtrans} as function of pressure.

3.2. Heterogeneous dynamics.

As shown above, the diffusion mechanism in alumina is realized by exchanging the nearest-neighbor atoms amongst coordination units (transition $\text{AlO}_x \rightarrow \text{AlO}_{x\pm 1}$). Considering the distribution of the transition $\text{AlO}_x \rightarrow \text{AlO}_{x\pm 1}$ (Fig.6) we find that the distribution transition for each atom in the simulation samples at pressure from 0 GPa to 20GPa is the Gaussian form with the peak at 240 transitions. It means that the average number of transitions per an atom is about 240 and it almost does not depend on pressure. Although the position of the peak of transition distribution does not depend on compression, the full width half maximum (FWHM) of transition distribution is depend on compression. At pressure of 0 GPa, the FWHM is about 360 transitions and at 20.47 GPa, it down to about 260 transitions. These distributions are the evidence of the spatially heterogeneous dynamics. From the distribution, it is clearly that there are coordination units that have the number of transitions very high. Conversely there are units that have the number of transitions very low. In the space, where contains coordination units with the number of transitions higher than the average value, then the atoms at that location have higher mobility and vice versa. In other word, the mobile atoms are sparse and dynamics are spatially heterogeneous. Mobile atoms assist their neighbors to become more mobile. This is dynamic facilitation and form mobile areas where there are atoms with high mobility

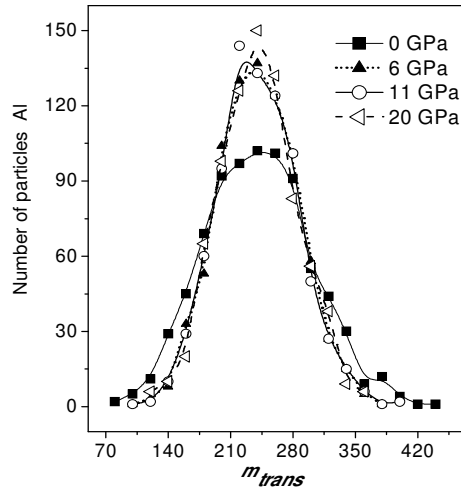


Fig. 6. The distribution transition $AlO_x \rightarrow AlO_{x\pm 1}$

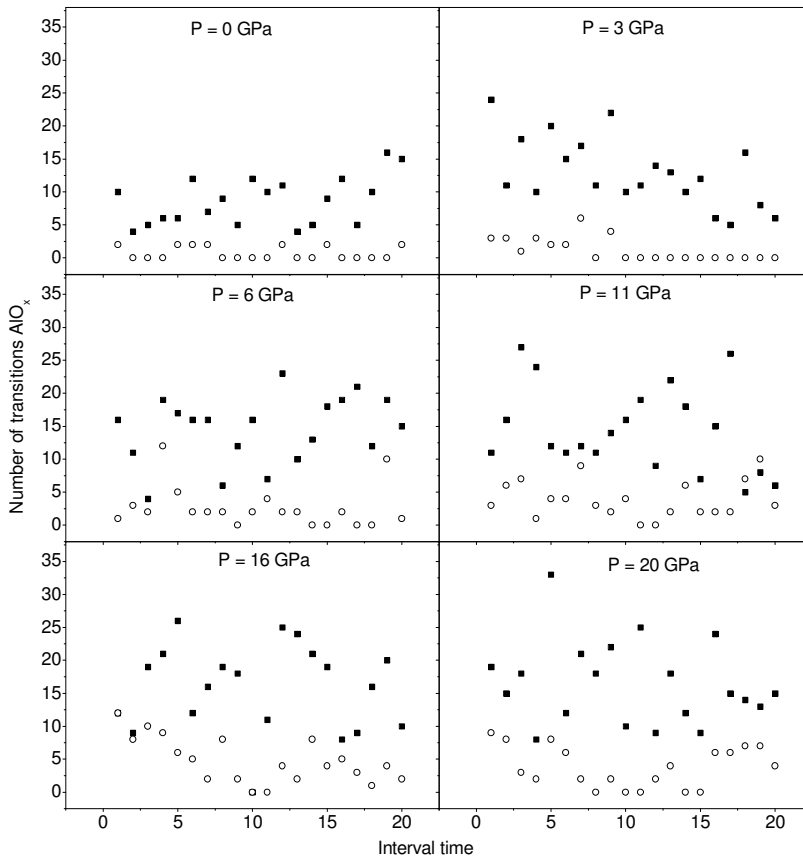


Fig.7. The evolution of transition $AlO_x \rightarrow AlO_{x\pm 1}$ for most fast and slow (MFP and MSP) with one particle Al.

4. Conclusions

The structural dynamics and diffusion mechanism in liquid Al_2O_3 are studied by the mean of molecular dynamic simulation. We trace the evolution of coordination units AlO_x ($x = 4, 5, 6$) in network structure of liquid Al_2O_3 over the simulation time. Simulation results have shown that each atom undergoes a series of stages where the coordination AlO_x is changed. The lifetime of coordination units is depend on pressure and varies from one to other units. The atomic diffusion in liquid Al_2O_3 is realized through the transitions $\text{AlO}_x \rightarrow \text{AlO}_{x\pm 1}$ (exchanging the nearest neighbor atoms amongst coordination units). Diffusion coefficient in liquid Al_2O_3 depends strongly on the lifetime of coordination units AlO_x (the rate of transition $\text{AlO}_x \rightarrow \text{AlO}_{x\pm 1}$). Simulation also shows that the low-pressure sample contains distinguished regions where $\text{AlO}_x \rightarrow \text{AlO}_{x\pm 1}$ occurs frequently and other ones where $\text{AlO}_x \rightarrow \text{AlO}_{x\pm 1}$ is rare, leading to spatially heterogeneous dynamics in the liquid.

Acknowledgement

The authors are grateful for support by the NAFOSTED Vietnam (grant No Grant No. 103.01-2011.32).

Reference

- [1] Hideyuki Mizuno and Ryoichi Yamamoto, Phys. Rev. E 82 (2010) 030501
- [2] L. Berthier and G. Tarjus ,Eur. Phys. J. E (2011) 34: 96
- [3] S. Franz, G. Parisi, F. Ricci-Tersenghi, and T. Rizzo, Eur. Phys. J. E (2011) 34: 102
- [4] M. Vogel, S. C. Glotzer, Phys. Rev. Lett., 92 (2004) 255901.
- [5] R . Yamamoto and A. Onuki, Phys. R ev. L ett. 81, 4915 (1998).
- [6] B . Doliwa and A. Heuer, J. Non-Cryst. Solids 307-310,32(2002).
- [7] C. Donati, J . F. Douglas, W. Kob, S. J. Plimpton, P. H. Poole,
- [8] U. Tracht, M. Wilhelm, A. Heuer, H. Feng, K. Schmid Rohr, and H.W. Spiess, Phys. Rev. Lett. 81, 2727 (1998)
- [9] E. R. Weeks, J. C. Crocker, A. C. Levitt, A. Schofield, andD. A. Weitz, Science 287, 627 (2000).
- [10] G. Adam and J. H. Gibbs, J. Chem. Phys. Vol. 43, No. 1 (1965), pp 139-146.
- [11] J. P. Garrahan and D. Chandler, Phys. Rev. Lett. 89, 035704 (2002).
- [12] C. A. Angell, J. Non-Cryst. Solids 131,13 (1991).
- [13] Y. Gebremichael, M. Vogel, and S. C. Glotzer, J. Chem.Phys. 120, 4415 (2004).
- [14] I. Levin and D. Brandon, J. Am. Ceram. Soc. 81, 1995 (1998).
- [15] P.K. Hung, N. T. T. Ha, and N. V. Hong, Correlation effect for dynamics in silica liquid, PHYSICAL REVIEW E 86, 041508 (2012)
- [16] F. Molnar etal. , Computer Physics Communications 181 (2010) 105.
- [17] P.K. Hung, and L.T. Vinh, J. Non-Crystal. Solids 352, 5531 (2006).
- [18] C. Landron, A.K. Soper, T.E. Jenkins, G.N. Greaves, L. Hennem, J.P. Coutures, J. Non-Cryst. Solids 293–295 (2001) 453.